

Photoinduced Formation of Microscopic Ordering and Macroscopic Pattern in Spiropyran-Containing Polyacrylate–Tetraoctylammonium Bromide Films

Shuizhu Wu,* Jiarong Lu, Fang Zeng, Yanan Chen, and Zhen Tong

Department of Polymer Science & Engineering, South China University of Technology, Guangzhou 510640, China

Received February 5, 2007; Revised Manuscript Received April 15, 2007

ABSTRACT: In this study, photoisomerizable polyacrylate containing spiropyran moieties was synthesized. By taking advantage of the photoinduced structural transformations of the spiropyran moieties, photoinduced microscopic ordering and eventually macroscopic patterns were formed in the polymer films consisting of spiropyran-containing polyacrylate (SPPA) and tetraoctylammonium bromide (TOAB). The patterns thus obtained are composed of concentric rings, which alternatively consist of macroscopic convex ridges and concave valleys, with the former being amorphous phases and the latter being ordered mesomorphous ones. It was found that the open-ring protonated merocyanine (MC) form of the spiropyran moieties, which is triggered by UV illumination, was crucial to the formation of mesomorphous structure and macroscopic patterns for this polymer–surfactant system. It is possible that the interaction between the MC form and TOAB leads to the formation of the microscopic ordering and macroscopic pattern in the polymer–TOAB films. This photoinduced macroscopic patterning in solid polymer–surfactant system could offer a new way for modulating and/or fabricating ordered supramolecular structure in macroscopic dimension by using light as a trigger.

Introduction

Materials with structure and accordingly properties that can be optically modulated are of great significance in a wide range of scientific research including optics, biotechnology and medicine.^{1,2} Some photoisomerizable (photochromic) compounds can be readily used to achieve this purpose, as they can be reversibly converted by light between two states with different spectroscopic properties.^{3–8} This attributes of these photoisomerizable compounds can then be used to modulate properties/structure at the molecular or supramolecular level by using light as a trigger.

In our previous studies, we found that unique mesomorphous structure and macroscopic patterns could be obtained by evaporating the organic solutions containing a surfactant tetraoctylammonium bromide (TOAB) and a polymer with polar groups like styrylthiophene or carboxyl.^{9,10} We supposed that the polar interactions between TOAB and the pendant polar groups along the polymer chain led to the mesomorphous structure and macroscopic patterns for the polymer–surfactant system.^{9,10} We were thinking that if we substitute these polar groups with photoisomerizable groups which can undergo structural transformations between low-polar (nonpolar) and polar (or ionic) forms, then possibly we could realize the formation of ordered structure in the polymer–TOAB system by using light as a trigger. On the other hand, we found that the polyacrylate with polar groups in its side chains could form the mesomorphous structure with TOAB, while the polyacrylate with no polar groups can not, however this result cannot directly prove that the polar groups on the polymer chains are absolutely the cause for the formation of ordered structure, since the polyacrylate with polar groups and the polyacrylate without polar groups are different polymers in terms of polymer

sequence and molecular weight, and the polymer sequence and molecular weight can also affect the formation of ordered structure. Thus, if we prepare *one* polymer sample with photoisomerizable groups and use the light to turn the nonpolar (or low-polar) groups into polar (or ionic) groups, then we can directly verify the role of polar groups in the structure formation.

Among the photoisomerizable species, spiropyran compounds are a promising family of photochromic materials. It is well-known that the spiropyran molecules can adopt one of two stable states: the open-ring state, known as the protonated (ionic) merocyanine (MC) form, and the closed-ring state, known as the low-polar spiro (Sp) form. Upon the irradiation of UV light, the spiropyran molecules adopt the MC form (coloration), while with visible light, they adopt the Sp form (decoloration).^{5,11–14} Photochromic spiropyran, which responds to external stimulation such as light to undergo this reversible structural interconversion and modulation of photophysical properties, could be the right photoisomerizable moieties which might help us achieve photoregulated ordered structure and verify the role of polar groups in the structure formation. Along this line of thinking, we synthesized the spiropyran-containing polyacrylate (SPPA), prepared the SPPA–TOAB films with or without UV illumination, and studied the pattern formation in these films. It is found that the open-ring protonated MC form of the pendant spiropyran moieties can lead to the formation of mesophase and macroscopic pattern; and only with the right amount of SPPA content in the polymer–surfactant system can the mesomorphous structure and macroscopic pattern be obtained in the solid films.

Experimental Section

Materials. *N,N'*-Dicyclohexylcarbodiimide, 4-(dimethylamino)-pyridine, 2-hydroxyethyl acrylate (HEA), methyl methacrylate (MMA), ethyl acrylate (EA), tetraoctylammonium bromide (TOAB), and 3-iodopropanoic acid were purchased from Sigma-Aldrich Co. 2,3,3-Trimethylindolenine was received from Acros Organics. 2-Hydroxyethyl acrylate, methyl methacrylate and ethyl acrylate were distilled before use. *N,N*-dimethylformamide (DMF), tetrahy-

* To whom correspondence should be addressed. E-mail: shzhwu@scut.edu.cn. Telephone: +86-20-83683721. Fax: +86-20-87114649.

dofuran (THF), acetone, 1,2-dichloroethane, ethyl methyl ketone, and methanol were analytically pure solvents, and the solvents were distilled before use.

Synthesis of Carboxyl-Containing Spiropyran (SpCOOH). During the synthesis process, all the reaction vessels were wrapped with aluminum foil, so as to ensure the reaction would proceed in the dark. The carboxyl-containing spiropyran 1-(β -carboxyethyl)-3',3'-dimethyl-6-nitrospiro (indoline-2',2[2H-1] benzopyran) (referred to as SpCOOH) was synthesized according to the literature.¹⁵ 2,3,3-Trimethylindolenine (0.06 mol), 3-iodopropanoic acid (0.06 mol), and ethyl methyl ketone (5 mL) were heated under nitrogen at 100 °C for 3 h. The resulting solid material was dissolved in water, and the solution was washed with chloroform. Evaporation of water gave 1-(β -carboxyethyl)-2,3,3-trimethylindolenine iodide (73% yield). The above-obtained iodide (0.04 mol), 5-nitrosalicylaldehyde (0.04 mol), and piperidine (3.8 mL, 0.04 mol) were dissolved in ethyl methyl ketone, and the red solution was refluxed for 3 h. When the reaction was allowed to stand overnight, the product precipitated as a yellow crystalline powder. This was filtered and washed with methanol to give the product SpCOOH (75% yield). ¹H NMR (400 MHz, deuterated DMSO, 25 °C, TMS) (ppm): 1.0–1.3 (2 CH₃), 2.6 (CH₂COO), 3.4–3.5 (CH₂N), 5.9–6.0 (olefinic protons, 2H), 6.6–8.2 (aromatic protons), 12.0 (COOH, hydrogen bonding). FT-IR (KBr): 3450 cm⁻¹ (ν_{OH}), 3020 cm⁻¹ (ν_{CH}), 3050 cm⁻¹–3080 cm⁻¹ (aromatic ν_{C-H}), 2970 cm⁻¹ and 2860 cm⁻¹ (aliphatic ν_{C-H}), 1710 cm⁻¹ ($\nu_{C=O}$), 1650 cm⁻¹ (aromatic ν_{C-C}), 1600 cm⁻¹ and 1380 cm⁻¹ (ν_{NO_2}), 1570 cm⁻¹ ($\nu_{C=C}$), 1480 cm⁻¹ (aliphatic δ_{C-H}), 1340 cm⁻¹ (ν_{C-N}), 1260 cm⁻¹, 1150 cm⁻¹ and 1030 cm⁻¹ (ν_{C-O-C}), 900–650 cm⁻¹ (aromatic δ_{C-H}).

Polymerization of Hydroxyl-Containing Polyacrylate (HPA). A 2.3 g sample of 2-hydroxyethyl acrylate was dissolved in dry dimethylformamide, and 9.0 g of methyl methacrylate and 9.0 g of ethyl acrylate were added to the solution. The polymerization was carried out in the presence of azobis(isobutyronitrile) (AIBN, 0.2 wt %) as an initiator. The polymerization medium was outgassed twice before heating and stirring at 70 °C for 240 h under nitrogen. Then the polymerization mixture was poured into cold methanol. The isolated copolymer was redissolved in THF and precipitated in cold methanol, filtered, washed with deionized water and finally dried under vacuum at 60 °C for 72 h. ¹H NMR (400 MHz, CDCl₃, 25 °C, TMS) (ppm): 5.0 (OH), 4.0–4.2 (O=COCH₂), 3.6–3.9 (–CH₂–OH, O–CH₃), 2.9–3.1 (CH–C=O), 2.20–1.40 (–CH₂–C), 1.30–0.70 (–CH₃). FTIR (KBr): 3520 cm⁻¹ (ν_{OH}), 2980 and 2870 cm⁻¹ (ν_{CH}), 1735 cm⁻¹ ($\nu_{C=O}$), 1480 cm⁻¹ (δ_{C-H}), 1380–1150 cm⁻¹ (ν_{C-O}), 850–750 cm⁻¹ (ν_{C-H}). $M_w = 8.3 \times 10^4$; polydispersity is 2.0.

Synthesis of Spiropyran-Containing Polyacrylate (SPPA). During the synthesis process, all of the reaction vessels were wrapped with aluminum foil, so as to ensure the reaction would proceed in the dark. The above SpCOOH (1.53 g) and 4.1 g of HPA were reacted in 30 mL of dry dimethylformamide (DMF) in the presence of 1.03 g of *N,N'*-dicyclohexylcarbodiimide and 0.06 g of 4-(dimethylamino)pyridine (DMAP) at 25 °C for 24 h. The mixture was then filtrated, and the filtrate was precipitated in methanol; afterward, the product was dissolved in DMF and reprecipitated in methanol for several times. Then the product was dissolved in acetone, and ether (acetone:ether = 1:7 in volume) was added to precipitate the product (about 80% yield). ¹H NMR (400 MHz, deuterated DMSO, 25 °C, TMS) (ppm): 0.7–1.3 (CH₃), 1.4–2.2 (–CH₂–C), 2.6 (CH₂COO), 3.1 (CH–C=O), 3.4–3.5 (CH₂N), 3.9–4.1 (O–CH₃), 4.5–4.7 (O=COCH₂), 5.9–6.0 (olefinic protons of spiropyran), 6.6–8.2 (aromatic protons). ¹³C NMR (400 MHz, deuterated DMSO, 25 °C, TMS) (ppm): 173 (C=O, connected to spiropyran moiety), 166 (C=O, EA and MMA unit), 159 (N–C–O–C aromatic), 146 (C–N–C–O aromatic), 140 (C–NO₂ aromatic), 115–125 and 136 (aromatic carbons of spiropyran), 127–128 (olefinic carbons of spiropyran), 106 (N–C–O), 60 (O–CH₂), 50–52 (O–CH₃), 30–33 (O=C–CH₂–CH₂–N), 26 (CH–C=O, chain backbone), 20–23 (C(CH₃)₂ spiropyran), 10–14 (CH₃ acrylate). FT-IR (KBr): 3450 cm⁻¹ (ν_{OH}), 3050 cm⁻¹ (aromatic ν_{C-H}), 2980 cm⁻¹ (aliphatic ν_{C-H}), 1740 cm⁻¹ ($\nu_{C=O}$),

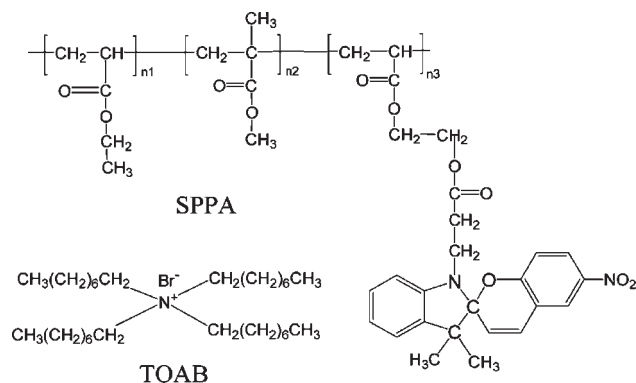


Figure 1. Molecular structure of the polymer SPPA and the surfactant TOAB.

1650 cm⁻¹ (aromatic ν_{C-C}), 1600 cm⁻¹ and 1380 cm⁻¹ (ν_{NO_2}), 1570 cm⁻¹ ($\nu_{C=C}$), 1480 cm⁻¹ (aliphatic δ_{C-H}), 1340 cm⁻¹ (ν_{C-N}), 1260 cm⁻¹, 1150 cm⁻¹ and 1030 cm⁻¹ (ν_{C-O-C}), 900–650 cm⁻¹ (aromatic δ_{C-H}). $M_w = 8.1 \times 10^4$; polydispersity is 2.1.

Film Preparation. As for the dissolution process, all the containers were wrapped with aluminum foil, so as to ensure the process will proceed in the dark. The polymer–surfactant films were prepared as follows: the surfactant and the polymer SPPA at a certain ratio were dissolved in an organic solvent (acetone, dichloroethane or toluene) to form a solution with the concentration of 6% by weight, a clear solution resulted, and then the solution was filtered through a 0.50 μ m Teflon filter. As for the films prepared in the dark, the above solution was cast on 2.0 cm \times 3.5 cm quartz glass substrate, and then a culture dish wrapped with aluminum foil was covered over the quartz glass substrate; afterward the films were allowed to dry in a thermostat at a constant temperature (25 °C). As for the films prepared under constant UV illumination, the above solution was first irradiated with UV light (365 nm, 16 W, irradiated for 10 min to ensure the close-ring spiropyran moieties were all turned into the open-ring form in the solution, similar experiments also indicated that this irradiation time can ensure the open-ring conversion¹⁶) and the solution quickly turned colored, then this colored solution was cast onto the quartz glass substrate, a culture dish was covered over the quartz glass substrate and UV light was kept irradiating over the quartz glass substrate (365 nm, 16W, at a distance of 5 cm), and it was allowed to dry under constant UV illumination in a thermostat at 25 °C. The film thickness was about 120 μ m.

Characterization. FT-IR spectra were measured by using Nicolet Magna 760 FT-IR spectrometer. ¹H NMR and ¹³C NMR spectra were recorded on a Bruker Avance 400 MHz NMR spectrometer. Molecular weight and molecular weight distribution was determined by Waters gel permeation chromatography with the 2410 RI detector, polystyrenes were used as standard. Polarizing micrographs were taken on a Zeiss Axiolab Polarizing microscope. Small-angle X-ray scattering (SAXS) measurements were performed on Philips X'Pert PRO X-ray diffractometer (Cu K α) (scattering vector $q = (4\pi/\lambda) \times \sin\theta$, 2θ is the angle between the incident light and the scattered light). Thermogravimetry (TG) was measured using a Netzsch TG 209 under nitrogen atmosphere at a heating rate of 10 °C/min from room temperature to 650 °C. UV–vis spectra were recorded on a Hitachi U-3010 UV–vis spectrophotometer at room temperature. Fluorescence spectra were recorded on a Hitachi F-4500 Fluorescence spectrophotometer.

Results and Discussion

Preparation and Photochromic (Photoisomerizable) Properties of SPPA. The synthesized spiropyran-containing polyacrylate (SPPA) is a random acrylate copolymer with pendant spiropyran groups (Figure 1). The polymer SPPA was synthesized by post-polymerization modification of hydroxyl-containing polyacrylate, which was conducted through esterification

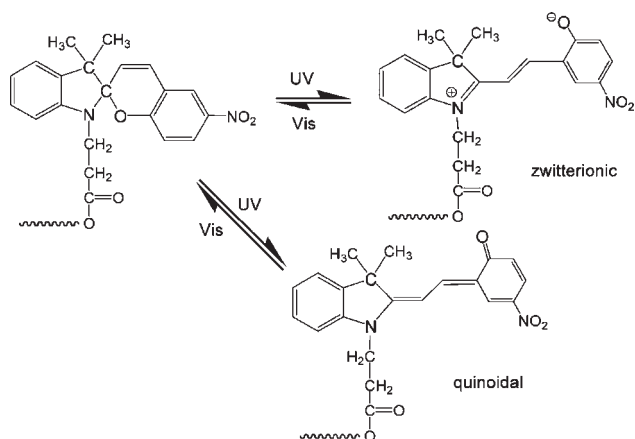


Figure 2. Nonpolar quinoidal and zwitterionic forms of spiropyran moieties on the polymer side chain.

between the pendant hydroxyl groups and the carboxyl-containing spiropyran. The content of spiropyran moieties in SPPA is estimated to be about 8.7 mol % based on NMR measurements. The molecular weight of the polymer, as characterized by gel permeation chromatography with polystyrene as the standard, is 8.1×10^4 with the polydispersity index of 2.1; and the glass transition temperature as determined by DSC for the polymer is 52 °C.

The UV–vis absorption spectra of the SPPA solutions as prepared in the dark (or upon visible light irradiation) and under UV illumination were measured (Figure S8). As for the solutions in the solvent acetone, 1,2-dichloroethane or toluene, without UV illumination, the solutions as obtained were colorless and showed no absorption in the 400–700 nm range. Upon UV illumination, the SPPA solution became colored (Figure S9) and showed strong absorptions in the range 400–700 nm (Figure S8): as for the solvent acetone, $\lambda_{\text{max}} = 568$ nm, and as for dichloroethane, $\lambda_{\text{max}} = 578$, while for toluene, $\lambda_{\text{max}} = 585$ nm. Under indoor lighting environment (visible light), the solutions returned to its colorless state, but the time required for the reversion process also differed for different solvents: as for the solvent acetone, the reversion process took about 16 min, and for dichloroethane, the reversion process took about 15 min, while for toluene, it took about 5 min. The phenomena that the absorption properties and the rates of reversion are solvent dependent are consistent with the results concerning spiropyran derivatives reported by other researchers.^{11,13} From the above experimental results, it is clear that, under UV illumination spiropyran moieties along the polymer chain undergo the cleavage of C–O bond and the ring-opening to produce the MC form, and the reversion process of the MC form to the SP form is more rapid in the polymer–toluene solution compared with that in the polymer–dichloroethane solution. This is because, the MC form of spiropyran moieties constitute a conjugated system that includes varying relative contributions of two canonical forms: nonpolar quinoidal and dipolar zwitterionic (Figure 2). Increasing the solvent polarity stabilizes the zwitterionic form over the quinoidal form.¹⁷ The MC–SP reversion is easier to occur for the quinoidal form than the zwitterionic form.¹⁷ Acetone (dielectric constant at 25 °C $\epsilon = 20.7$) and dichloroethane ($\epsilon = 10.5$ at 25 °C) have a higher polarity than toluene ($\epsilon = 2.24$). Therefore, when the polymer was dissolved in a higher polar solvent, there exists a more zwitterionic MC form than the nonpolar quinoidal MC form.

Macroscopic Patterns Formed by Surfactant and SPPA.

The polymer and TOAB were dissolved in the solvent dichlo-

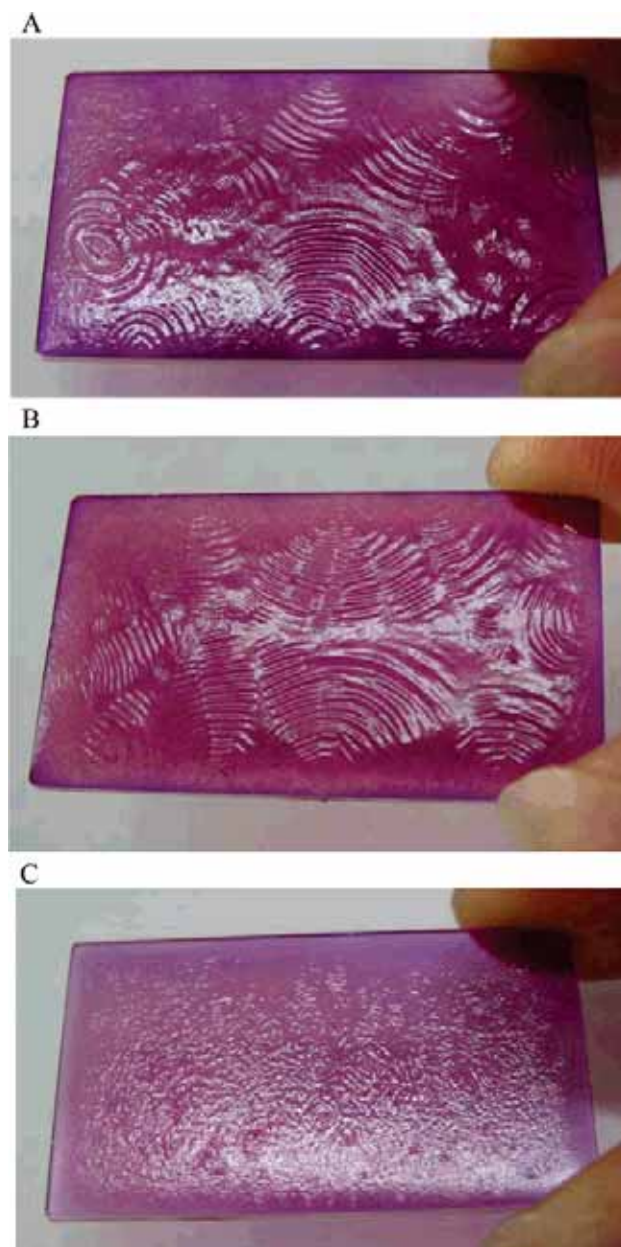


Figure 3. Photographs of the patterns formed in the SPPA–TOAB solid films (SPPA 50 wt %) prepared under constant UV illumination: (A) from acetone solution; (B) dichloroethane; (C) toluene.

roethane, acetone, or toluene with an appropriate polymer to surfactant ratio, a transparent solution was obtained; all the containers for the dissolution were wrapped with aluminum foil, so as to ensure the dissolution process proceeded in the dark. Under appropriate conditions, the macroscopic pattern composed of millimeter-scale concentric rings appeared during the solvent evaporation under constant UV illumination. The photographs of the patterns formed in the SPPA–TOAB solid films prepared under constant UV illumination are shown in Figure 3. While the photographs of the SPPA–TOAB films formed in the dark are shown in Figure 4. The as-obtained SPPA–TOAB film which was formed under constant UV illumination appeared purplish red (Figure 3A); after being stored in ordinary indoor lighting environment for 1 day, the film faded a little and remained a bit purplish red (Figure S10); when the film was reirradiated by UV light, no color change occurred. As for the as-obtained SPPA–TOAB film which was prepared in the dark

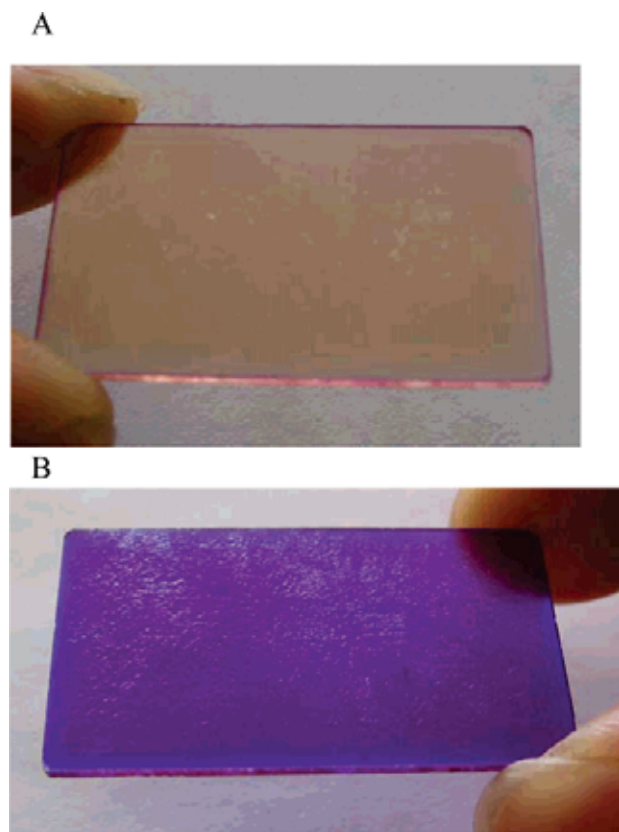


Figure 4. Photographs of the SPPA-TOAB solid films (SPPA 50 wt %) formed from acetone solution: (A) as-obtained SPPA-TOAB film formed in the dark; (B) the same film in part A upon UV light irradiation.

(Figure 4A), the film looked slightly yellow and storing in ordinary indoor lighting environment led to no color change. However, when this film was illuminated by UV light, it quickly turned purple (Figure 4B), similar to the color of pure SPPA film formed under constant UV illumination (Figure S10), and it returns to its slight yellow state under visible light illumination. This could imply that the polymer in this film (formed in the dark) exists in a state similar to that in the pure SPPA film. The experimental phenomena could be explained as follows: Under UV illumination, spiropyran moieties on the polymer side chains turned to the ring-opening MC form (ionic or polar), the polar interactions between the ionic or polar MC form with TOAB lead to the formation of mesomorphous structure, and this surfactant-rich mesomorphous domains and the polymer-rich amorphous domains in the mixture of polymer-surfactant-solvent underwent phase separation during the solvent evaporation, resulting in the formation of macroscopic patterns on the polymer-surfactant film.¹⁰ With the gradual evaporation of the solvent, the patterns were kinetically frozen and they could retain their shape after the UV irradiation was removed, thus the formation of pattern is irreversible. While for the films prepared in the dark, most of the spiropyran moieties remain the low-polar close-ring SP form in the solid film, there is no strong polar interaction between polymer side chains and surfactants, which is essential for the formation of mesomorphous structure. Hence, no pattern was observed during the solvent evaporation.

As for the color change of the solid films, we observed that the polymer-surfactant films formed under UV illumination displayed purplish red and exposed the films under ordinary indoor light or under further UV irradiation could not change

the color again, reflecting the fact that the color change is not reversible for the film. However, for the films of polymer-surfactant formed in the dark and the films of pure polymer, we could clearly observed reversible color change, e.g., under UV irradiation, the films turned into purple and under irradiation of visible light, the films turned into purplish red. This result indicates that there exists strong interaction between ionic ring-open form of spiropyran moieties and the surfactant molecules, and the interaction hinders the spiropyran moieties returning to its close-ring structure; While there is no strong interaction between close-ring form of spiropyran moieties and surfactant molecules, and the polymer-surfactant films formed in the dark showed reversible color change upon UV or visible light irradiation. And we think this experiment can provide direct evidence that the polar interaction is the main driving force for the formation of mesomorphous structure and the macroscopic patterns.

From Figure 3, it is also can be seen that, with the same SPPA content in the polymer-surfactant system and under constant UV illumination, a macroscopic pattern could be formed in the films prepared with the solvent acetone and dichloroethane (Figure 3, parts A and B), while almost no macroscopic pattern could be formed in the film prepared with the solvent toluene (Figure 3C).

Effects of Polymer-Surfactant Weight Ratio and Solvent on Pattern Formation. The weight ratio of polymer to surfactant in the solution is also critical to the pattern formation. For the SPPA-tetraoctylammonium bromide (TOAB) film prepared under constant UV illumination, no matter what solvent was used, as the weight percentage of the polymer was low (10 wt %), no macroscopic pattern appeared in the solid polymer-surfactant film as the solvent evaporates. As the weight percentage of polymer reached 30% in the solid film, poorly formed patterns could be observed, and a large and well-formed pattern could be observed as the polymer content was increased to around 50 wt % in the solid film when acetone or dichloroethane was used as the solvent (under constant UV light illumination), as shown in Figure 3. When the amount of polymer in the solid film was too high (80 wt % or higher), no macroscopic pattern could be observed as well.

In addition, several solvents with different polarities were also employed to prepare the SPPA-TOAB solid films. As for the relatively high polar solvents (e.g., acetone and dichloroethane with a dielectric constant of 20.7 and 10.5, respectively), when the polymer content is between 50 and 60 wt %, well-formed macroscopic patterns could appear as the solvent evaporated under constant UV illumination. While for the relatively low-polar solvent toluene (dielectric constant equals 2.24), almost no macroscopic patterns could be generated under constant UV irradiation. We suppose, the interactions between the ionic or polar ring-opening MC form moieties (which were induced by UV illumination) along the polymer chain and the surfactant TOAB is necessary for this structure formation. In the solvent with higher polarity, most of the MC form spiropyran moieties along the polymer chain exist in the zwitterionic form (polar) under UV illumination; hence, there are stronger interactions between the polymer and the surfactant TOAB, which in turn lead to the structure formation. However, in the solvent with lower polarity like toluene, most of the pendant spiropyran moieties along the polymer chain exist in the nonpolar quinoidal form under UV irradiation and there is no sufficient interaction between the polymer and the surfactant; hence, no ordered structure can be observed. This result also is consistent with the photochromic (photoisomerizable) properties

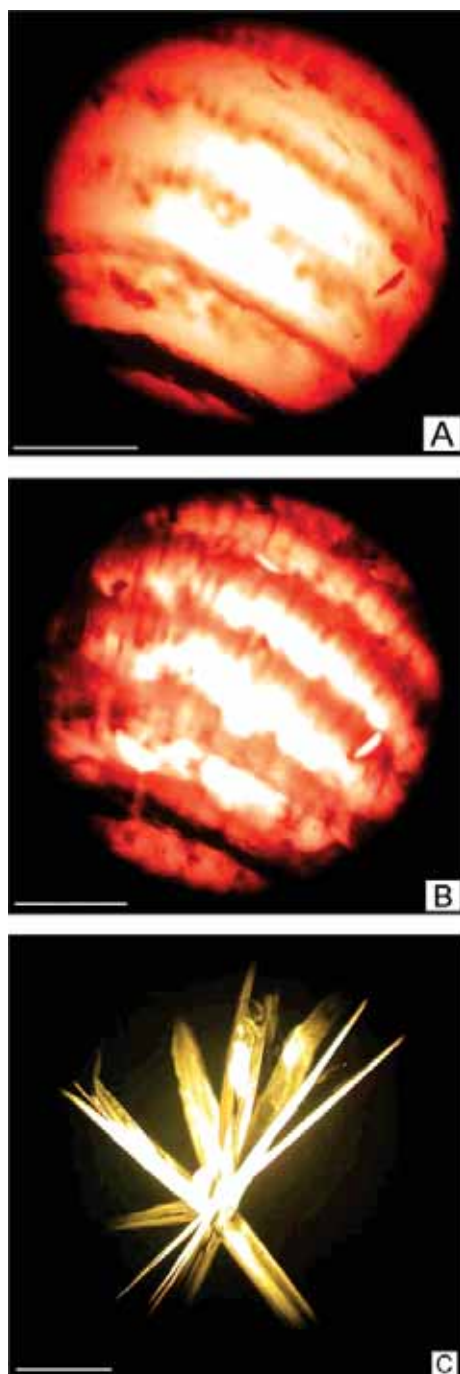


Figure 5. Photographs for the SPPA–TOAB films (formed from acetone solution under constant UV illumination, SPPA 50 wt %) observed on polarizing optical microscope: (A) a part of a pattern under parallel-polarized light (scale bar 0.5 mm); (B) the same part of the pattern as that in Figure 5A under perpendicular-polarized light; (C) a part of the film formed by acetone solution of pure TOAB under perpendicular-polarized light.

of the polymer SPPA in the solvents with different polarities. Hence, the pattern was controllable to some extent by adjusting the polymer–TOAB ratio and the type of solvent used.

Polarizing Optical Micrographs. The morphologies of the macroscopic patterns were studied by using the polarizing optical microscope with some small rings in the pattern. Figure 5 shows the morphology for a same part of a pattern under parallel-polarized light and perpendicular-polarized light respectively. With the comparison of Figure 5A and Figure 5B,

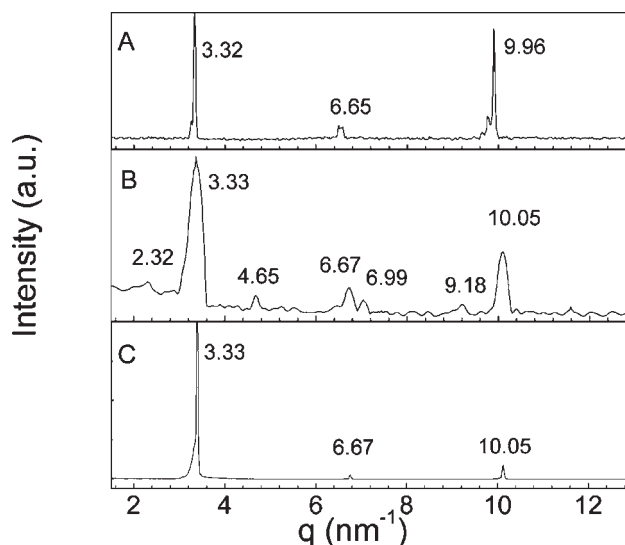


Figure 6. SAXS profiles: (A) pure surfactant TOAB cast from acetone; (B) concave region from the SPPA/TOAB film cast from acetone and prepared under constant UV illumination with the polymer content of 50 wt %; (C). SPPA/TOAB film cast from acetone and prepared in the dark with a polymer content of 50 wt %.

it can be seen that each brighter stripe in Figure 5A corresponds to one bright stripe in Figure 5B. Under the parallel-polarized light (similar to unpolarized light), the thinner regions of a film absorb less light, hence the brighter stripes in Figure 5A represent the concave valleys. However, in Figure 5B, bright stripes represent anisotropic structure. Therefore, it can be found that only the concave valleys of the film can transmit the perpendicular-polarized light, while the ridges cannot; this indicates that the convex ridges mostly contain the isotropic (amorphous) structure, while the concave valleys mainly comprise the ordered anisotropic structure. Similar to what we have observed in our previous study,^{9,10} as the polarizers were rotated (the angle between the two polarizers was varied from 0° to 90°), the concave regions in a pattern always correspond to the bright stripes, and the convex regions correspond to the dark stripes (Figure S12). Therefore, it is confirmed that the dark stripes (the convex ridges) represent the amorphous structure, while the bright stripes (the concave valleys) represent the ordered anisotropic structure. For comparison, the photograph for a film cast from acetone solution of pure surfactant TOAB is shown in Figure 5C, under the perpendicular-polarized light, the highly crystalline structure of the surfactant is very much different from the mesomorphous structure in polymer/TOAB films.

Small-Angle X-ray Scattering Profiles. The investigations on ordered structures in the macroscopic pattern with small-angle X-ray scattering (SAXS) measurement are illustrated in Figure 6, in which the scattering intensities are given as a function of the scattering vector q (nm^{-1}). The SAXS measurements were conducted for the film prepared in the dark, and for both the convex region and the concave region in the film formed under constant UV illumination. It is well-known that different microphase structures will exhibit different peak position ratios in the SAXS profile.^{18–22} For example, the ratio of the q values at the scattering maxima should be 1, 2, 3, 4, ... for lamellae and 1, $(3)^{1/2}$, $(4)^{1/2}$, $(7)^{1/2}$, $(9)^{1/2}$, ... for cylinders in a hexagonal array. A polymer–surfactant system can also exhibit multiple SAXS peaks due to its periodic microscopic structure having a long-range order. Information on the morphology can be obtained from the relative positions of these

peaks. They can exhibit specific spatial relationships depending on the shape of the microdomain structure.^{19,23–25} It can be seen that for the pure surfactant (Figure 6A), there are three sharp peaks in the SAXS profile and the positions of these peaks are 3.32, 6.65, and 9.96 nm⁻¹, and this relative position of peaks is close to that of the lamella structure. For the polymer–TOAB film formed in the dark (Figure 6C), the SAXS profile is similar to that of the pure surfactant, indicating that the polymer SPPA and TOAB exist in the state of pure mixture in this solid film. While for the convex region in the SPPA–TOAB film prepared under constant UV illumination, no peaks can be observed in the SAXS profile, indicating that the convex ridge in the macroscopic pattern mainly contain the amorphous region (Figure S11). For the concave region in the SPPA–TOAB film (SPPA content 50% by weight) prepared under constant UV illumination (Figure 6B), there were 6 peaks in the SAXS profile with their peak positions of 2.32, 3.33, 4.65, 6.67, 6.99, 9.18, and 10.05 nm⁻¹, indicating that new structure was formed, and the scattering is generated by a superposition of two different lamellar systems, one with a period around $2\pi/3.32$ nm and one with a period around $2\pi/2.32$ nm (newly formed structure).

The small-angle X-ray scattering investigations further prove that the ordered structure observed on the polarizing optical microscope is the mesomorphous phase formed by the surfactant chain packing in the polymer–surfactant system.

On the basis of the above investigations and observations, it was understood that in general the pattern formation is a solvent evaporation induced phase separation. Thermodynamically, during the evaporation of solvent under constant UV irradiation, the polymer–surfactant interactions led to the formation of mesomorphous structures. In the polymer–surfactant solution, after the formation of the mesophase structure between the polymer and surfactant, as the solvent further evaporated, phase separation occurred, consequently surface undulation formed on the polymer–surfactant film. On the other hand, the kinetic trapping of structures occurred as a result of reduced mobility caused by solvent evaporation. Because of the effect of solvent evaporation, the patterns obtained by solution-casting may not be in thermodynamic equilibrium and relaxation toward equilibrium may be hindered by kinetic barriers formed by the nonequilibrium phase morphology, although the patterns are stable, kinetically “frozen” structures.^{26,27} The following forces could be responsible for surface undulation: the large interfacial tension between the surfactant–polymer mesomorphous phase and the polymer amorphous phase and/or the evaporation-induced convection.

Thermal Properties. The thermal properties of the SPPA–TOAB film were characterized by using TG, and the TG thermograms are shown in Figure 7. The temperature at which the weight loss starts is referred to as the initial degradation temperature, T_{id} , and the temperature where the weight-loss rate becomes maximal is defined as the maximum degradation temperature, T_d . A two-step weight-loss process is observed for the SPPA–TOAB system. The first weight-loss step occurs below 290 °C mainly due to the loss of the TOAB moieties in the system. The second weight-loss step at about 400 °C is due to the degradation of SPPA in the system because the rapid weight-loss of pure SPPA was observed at 404 °C. In addition, the T_d of the second weight-loss step does not show an obvious dependence on the SPPA content in the system (Table 1), which further supports our conclusion that the TOAB have already been lost during the first degradation step. T_d and T_{id} for the first degradation step are listed in Table 1. It can be seen that, for the SPPA–TOAB system (SPPA 50 wt %) prepared under

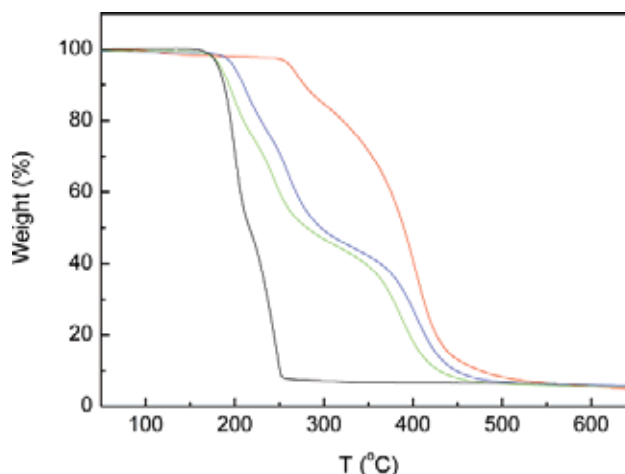


Figure 7. TG thermograms: red line, pure SPPA polymer; blue line, SPPA–TOAB film (SPPA 50 wt %) prepared under constant UV illumination (sample from the mixture of both the concave and convex regions); green line, SPPA–TOAB film (SPPA 50 wt %) prepared in the dark; black line, pure TOAB.

Table 1. The Initial Degradation Temperature T_{id} and the Maximum Degradation Temperature T_d

sample	first degradation phase		second degradation phase
	T_{id} (°C)	T_d (°C)	T_d (°C) ^a
TOAB	155.0	198.0	
SPPA–TOAB film prepared under UV illumination (SPPA 50 wt %)	180.0	208.0	401.0
SPPA–TOAB film prepared under UV illumination (SPPA 60 wt %)	182.0	209.0	402.0
SPPA–TOAB prepared in the dark (SPPA 50 wt %)	156	198.5	400.0

^a The maximum degradation temperature of the pure SPPA is 404 °C.

constant UV illumination, T_d of the first degradation step increases to 208 °C compared with the pure TOAB with T_d = 198 °C. Obviously, the thermal stability of TOAB in the polymer–surfactant is raised by about 10 °C compared with pure TOAB. While the T_{id} of this polymer–surfactant system (SPPA 50 wt %) is increased to 180 °C compared with the pure TOAB with T_{id} = 155 °C. This enhancement should be attributed to the strong electrostatic interaction between TOAB and SPPA accompanying the hydrophobic interaction among the TOAB tails and the polymer backbone in the system, which greatly restricts the mobility of TOAB molecules and leads to an ordered arrangement in the system.

As for the SPPA–TOAB films (SPPA 50 wt %) prepared in the dark, during the first degradation phase, T_d is 156 °C and T_{id} is 198.5 °C, which are similar to those of the pure surfactant TOAB. This result indicates that this SPPA–TOAB system (prepared in the dark) consists of pure mixture of the polymer and the surfactant, and no strong interactions exist in the system, which is consistent with the above SAXS measurement results.

Conclusions

Photoinduced microscopic structure and macroscopic pattern were obtained with tetraoctylammonium bromide (TOAB) and the polyacrylates with pendant spiropyran groups by taking advantage of the photoinduced structural transformations of the spiropyran moieties. The driving forces for the structure formation could be the polar interaction between the open-ring protonated MC form of the pendant spiropyran moieties and TOAB in the polymer–surfactant system. This study could offer

a strategy for the rational design of the polymer/ surfactant system that could lead to ordered supramolecular structure in macroscopic dimension by using light as a trigger.

Acknowledgment. This work was supported by NSFC (Project Nos. 50473035 and 50573023) and NCET.

Supporting Information Available: Figures showing FTIR spectra, ^1H NMR spectra, ^{13}C NMR spectrum, UV-vis absorption spectra of the SPPA solutions, photographs of the SPPA solutions prepared in the dark or upon UV illumination, photographs of the SPPA-TOAB films and the pure SPPA films formed from acetone solution, and photographs of a part of the pattern on polarizing optical microscope as the polarizers are rotated. This material is available free of charge via the Internet at <http://pubs.acs.org>.

References and Notes

- Irie, M.; Kobatake, S.; Hirochi, M. *Science* **2001**, *291*, 1769–1772.
- Bossi, M.; Belov, V.; Polyakova, S.; Hell, S. W. *Angew. Chem., Int. Ed.* **2006**, *45*, 1–5.
- Andreasson, J.; Straight, S. D.; Kodis, G.; Park, C. D.; Hambourger, M.; Gervaldo, M.; Albinsson, B.; Moore, T. A.; Moore, T. A.; Gust, D. *J. Am. Chem. Soc.* **2006**, *128*, 16259–16265.
- Such, G. K.; Evans, R. A.; Davis, T. P. *Macromolecules* **2006**, *39*, 9562–9570.
- Bahr, J. L.; Kodis, G.; Garza, L.; Lin, S.; Moore, A. L. *J. Am. Chem. Soc.* **2001**, *123*, 7124–7133.
- Uchida, E.; Kawatsuki, N. *Macromolecules* **2006**, *39*, 9357–9364.
- Sumaru, K.; Kameda, M.; Kanamori, T.; Shinbo, T. *Macromolecules* **2004**, *37*, 4949–4955.
- Trajkovska, A.; Kim, C.; Marshall, K. L.; Chen, S. H. *Macromolecules* **2006**, *39*, 6983–6989.
- Wu, S. Z.; Zeng, F.; Zhu, H. P.; Tong, Z. *Macromolecules* **2006**, *39*, 2606–2613.
- Wu, S. Z.; Zeng, F.; Zhu, H. P.; Luo, S. J.; Ren, B. Y.; Tong, Z. *Macromolecules* **2005**, *38*, 9266–9274.
- Berkovic, G.; Krongauz, V.; Weiss, V. *Chem. Rev.* **2000**, *100*, 1471–1753.
- Such, G. K.; Evans, R. A.; Davis, T. P. *Macromolecules* **2006**, *39*, 1391–1396.
- Suzuki, T.; Kato, T.; Shinozaki, H. *Chem. Commun.* **2004**, 2036–2037.
- Such, G.; Evans, R. A.; Yee, L. H.; Davis, T. P. *J. Macromol. Sci. - Polym. Rev.* **2003**, *C43*, 547–579.
- Fissi, A.; Pieroni, O.; Ruggeri, G.; Ciardelli, F. *Macromolecules* **1996**, *28*, 302–309.
- Rosario, R.; Gust, D.; Hayes, M.; Springer, J.; Garcia, A. A. *Langmuir* **2003**, *19*, 8801–8806.
- Wojtyk, J. T. C.; Wasey, Kazmaier, A.; P. M.; Hoz, S.; Buncel, Erwin. *J. Phys. Chem. A* **2000**, *104*, 9046–9055.
- Thunemann, A. F. *Adv. Mater.* **1999**, *11*, 127–130.
- Thunemann, A. F. *Prog. Polym. Sci.* **2002**, *27*, 1473–1572.
- Thunemann, A. F.; Muller, M.; Dautzenberg, H.; Joanny, J. F.; Lowen, H. *Adv. Polym. Sci.* **2004**, *166*, 113–171.
- Zhou, S. Q.; Hu, H. B.; Burger, C.; Chu, B. *Macromolecules* **2001**, *34*, 1772–1778.
- Kotz, J.; Kosmella, S.; Beitz, T. *Prog. Polym. Sci.* **2001**, *26*, 1199–1232.
- Sakurai, S.; Tanaka, K.; Nomura, S. *Macromolecules* **1992**, *25*, 7066–7068.
- Zhang, S.; Eugene, M. T.; Donald, A. M. *Macromolecules* **2004**, *37*, 390–396.
- Chu, B.; Hsiao, B. S. *Chem. Rev.* **2001**, *101*, 1727–1761.
- Petersson, M.; Loren, N.; Stading, M. *Biomacromolecules* **2005**, *6*, 932–941.
- Walheim, S.; Boltau, M.; Mlynek, J.; Krausch, G.; Steiner, U. *Macromolecules* **1997**, *30*, 4995–5003.

MA070318C